buildings

MDPI

Article

Colored BIPV with Multilayer Interference Coatings: Electrical Performance Assessment and Development of a Tailored Color Quantification Method in Outdoor Environment

Mustafa Abed Alrhman [1,*], Raymond Dresens [1], Roberto Habets [2,3], Peter van Nijnatten [4], Serge Timmermans [4], Daniel Mann [2,3,5], Cindy P. K. Yeung [2,3], Pascal Buskens [2,3,5], Chiraag Reddy [6], Zeger Vroon [1] and Fallon Colberts [1,*]

1 Engineering Department, Zuyd University of Applied Sciences, Nieuw Eyckholt 300, 6400 AN Heerlen, The Netherlands
2 The Netherlands Organisation for Applied Scientific Research (TNO), High Tech Campus 25, 5656 AE Eindhoven, The Netherlands
3 Brightlands Materials Center, Urmonderbaan 22, 6167 RD Geleen, The Netherlands
4 OMT Solutions, High Tech Campus 9, 5656 AE Eindhoven, The Netherlands
5 Design and Synthesis of Inorganic Materials (DESINe), Institute for Materials Research (IUMAT), Hasselt University (UHasselt), Agoralaan Building D, B-3590 Diepenbeek, Belgium
6 Kameleon Solar, Belder 1, 4704 RK Roosendaal, The Netherlands
* Correspondence: mustafa.abedalrhman@zuyd.nl (M.A.A.); fallon.colberts@zuyd.nl (F.C.)

Abstract

Building-integrated photovoltaics (BIPV) have achieved a high level of technical maturity. In spite of that, the installed capacity remains limited. To stimulate the integration of solar panels in the built environment, aesthetical features like color and freedom in size and shape are of key importance for architects and building owners. Multilayer interference coatings are an attractive coloring technique for solar panels, as they are known for their high solar transmission and tuneable reflection peak. The latter gives rise to an intense metallic reflection color. In this study, the outdoor performance of colored versus non-colored BIPV panels was investigated, and a method has been developed to measure the color variation of the solar panels with respect to outdoor conditions, viewing angles and tilt angles of the setup. A limited performance loss of 15% was measured for colored solar panels compared to their black counterparts, caused by a reduction in generated photocurrent due to light loss. Outdoor color measurements showed that the cloudiness of the sky and the tilt angle of the setup are key parameters causing a color variation from yellow-green to blue-green. In addition, the developed method and tailored measurement setup have proven their value in quantifying color appearance of colored BIPV in realistic and varying outdoor conditions.

Keywords: building-integrated photovoltaics (BIPV); outdoor monitoring; multilayer interference coating; electrical performance; color quantification

Check for updates

Academic Editor: Bo-Tao Huang

Received: 11 May 2026
Revised: 2 June 2026
Accepted: 8 June 2026
Published: 12 June 2026

Copyright: © 2026 by the authors. Licensee MDPI, Basel, Switzerland. This article is an open access article distributed under the terms and conditions of the Creative Commons Attribution (CC BY) license.

1. Introduction

As the operation of the built environment is responsible for 40% of the energy use and related greenhouse gas (GHG) emissions, it remains an important and strategic topic of research for decarbonization of our environment and economy [1]. Reducing energy use in the built environment is one of the pillars described in the Green Deal, Fit for 55 and REPowerEU proposals, aiming to reach quantitative goals in the EU Climate Law to reduce

EU GHG emissions by at least 55% by 2030 (compared to 1990 levels) and become climate-neutral by 2050 [2–4]. The Trias Energetica describes three important strategies to reduce energy demand of the built environment: (i) minimize energy demand, (ii) implement sustainable energy sources, and (iii) cover remaining energy demand in an efficient way [5]. Since the 20th century, minimizing energy demand of the built environment is a key topic of research, starting with the introduction of the double-glazed window in 1938. Nowadays, research is focused on, for example, smart window coatings that can minimize the energy demand for heating and cooling [6,7] or circular materials for building skin insulation [8,9]. The second aspect of the Trias Energetica covers the generation of renewable electricity and heat by well-known techniques, such as solar panels, solar thermal collectors, wind energy, or ground-coupled heat exchangers.

Over the last decade, the installed photovoltaic (PV) capacity has increased massively worldwide with decreasing installation costs. Nowadays, the availability, reliability and affordability of energy are very important aspects to maintain living comfort in the built environment, in which solar electricity can have a significant impact [10,11]. It is expected that electricity generated by solar panels will surpass the worldwide renewable electricity generation from wind, with wind and solar energy combined accounting for 30% of the renewable electricity generation in 2030 [12]. Many studies describe the importance of buildings in increasing the installed PV capacity [13–16]. K. Bódis et al. [17] show that EU rooftops could potentially produce 680 TWh of electricity, being 24% of the current electricity consumption.

Although the standard, rigid, silicon solar panels are very suitable for application on existing rooftops, full exploitation of a building skin requires the development of innovative aesthetic, customizable and flexible solutions. Today, building-integrated PV (BIPV) has reached a high level of technical maturity and proved its potential in the energy transition as a hybrid construction and energy component. Although many BIPV projects have been a great success from a technical perspective, it continuous to occupy a niche market. Strong collaboration, communication and coordination are required in the multidisciplinary field of architecture and solar energy, along with a broad and custom range of aesthetical variations. Choice in color is one of the aesthetical parameters required by architects to integrate solar energy in the building skin [18–21].

Various technical approaches for colored solar panels have been investigated, for example, color filters applied to the glass–air interface or glass–encapsulant interface [22,23], front glass coated with multilayer interference coatings [24–27], or pigments added to the encapsulant. Multilayer interference coatings have gained a lot of attention, since the color coating does not interfere with the state-of-the-art solar panel production methods, this concept provides the ability to tune the color by simply changing refractive indices and/or layer thickness, and can be combined with other technologies, such as anti-fouling or anti-glare properties [28,29]. The concept of interference coatings for colored solar panels has been widely explored on lab samples and applied in several commercial products like ColorQuant^{TM} and Kromatix, where the interference coatings are applied to glass by screen printing and plasma deposition, respectively [18,30,31]. Vibrant colors with many color variants, a long lifespan and a high solar module performance demonstrate the great potential of interference coatings for aesthetic solar panels. In this research, colored interference coatings are manufactured by sol–gel chemistry and applied from solution using a dip coat process, which is not widely explored for the production of colored solar panels. Nonetheless, the sol–gel method is a very mature technology and has proven its advantages in low-cost, fast and versatile processing of coatings, low-temperature processing, incorporation of additives, and is applicable to large-scale production facilities like dip coating, roller coating and slot–die coating [32–34]. Researchers at TNO-Brightlands

Material Center optimized a sol–gel coating formulation which was dip-coated into a stack of SiO_2 and TiO_2 interference layers. R. Habets et al. reported that these sol–gel interference coatings can be prepared in various colors with a reduced solar light transmission of 20% over the whole solar spectrum [35].

Assessment of the electrical and aesthetical properties of colored solar panels comprising sol–gel coatings applied from solution by dip coating under realistic outdoor conditions is essential for the industrialization of colored solar panels. Many studies have focused on the optical properties of color coatings on a lab scale with standardized methods and equipment [22,23,25,26,29]. Color quantification of aesthetical solar panels in a realistic outdoor environment is less well investigated and applied. Therefore, this research addresses the following two questions: (i) which measurement setup and method is required to assess the performance and aesthetics of colored BIPV with multilayer interference coatings in an outdoor environment? and, (ii) which factors influence the electrical performance output and aesthetics of colored BIPV with multilayer interference coatings? To answer these research question, a tailored outdoor measurement setup has been designed and realized that gives insights into the effect of outdoor conditions, tilt angle of the colored solar panels, and viewing angle on the variation in color appearance of the multilayer interference-coated BIPV panels. A measurement method has been developed to analyze the color appearance of the colored solar panels and interpret the data. The tailored measurement setup and measurement method are unique in quantifying color in a realistic outdoor environment and can be of interest in, for example, assessing angular dependent color variation or effects of weathering on color appearance. In addition, the tailored measurement setup gives the ability to assess the electrical performance of the colored and non-colored solar panels with various tilt angles. An electrical monitoring setup was designed and implemented, which allowed to compare the power output of both solar panels in one-minute data resolution with respect to the environmental conditions.

2. Materials and Methods

Solar panels: four color-coated and four uncoated solar panels have been produced in a collaboration between Kameleon Solar and TNO-Brightlands Material Center. The solar panels have a dimension of 800 mm by 1080 mm and contain 24 monocrystalline silicon cells connected in series. Details on the solar panel design and standard test condition (STC) performance can be found in Supporting Information S1. Glass sheets (4 mm thickness, low-iron, Pilkington Optiwhite) coated with a three-layer SiO_2/TiO_2 interference coating have been produced by TNO-Brightlands Material Center in collaboration with Prinz Optics by a sol–gel dip coating process. The coatings were applied on 1150×850 mm^2-sized glass plates. Prior to production of the colored solar panels, in total 7 cm was cut from the top and bottom edge and 5 cm from the left and right edge of the coated glass plate to remove edge effects and thickness inhomogeneities resulting from the dip coating process. After production of the colored solar panels, the color homogeneity over the full surface was analyzed via color measurements on 4 spots using a handheld spectrophotometer (Konica Minolta CM-23d) (Figure 1, Table 1). Reference non-colored solar panels were produced using SGG ALBARINO T solar glass from Saint Gobain, which is low-iron, extra-clear, two-sided finely structured patterned solar glass.

Angle-dependent transmission: Transmission measurements were performed with a PerkinElmer Lambda 1050 spectrometer in combination with the Total Absolute Measurement System (TAMS) detector, developed by OMT Solutions. An enhanced Si/InGaAs sphere detector was used with a measurement range of 200–2500 nm. The angular range for transmission measurements is 0–85° and measurements were taken at the angles of

incidence 0°, 15°, 30°, 45°, and 60°. An aligned broadband polarizer was used in the sample stage to measure the transmission of s- and p-polarized light.

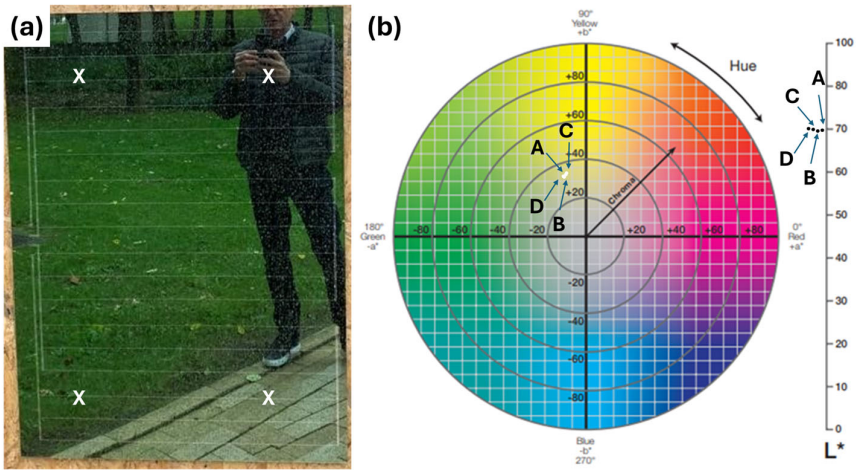

Figure 1. (**a**) Colored solar panel with measurement spots for color measurements and (**b**) obtained measurement results within the CIELAB color space (A = top left x; B = top right x; C = bottom left x; D = bottom right x).

Table 1. CIELAB color coordinates obtained from 4 different measurement spots (top left = 20 cm from top edge and 25 cm from left edge; top right = 20 cm from top edge and 26 cm from right edge; bottom left = 20 cm from bottom edge and 25 cm from left edge; bottom right = 20 cm from top bottom and 26 cm from right edge) on one colored solar panel.

Spot	l	a	b	Color
Top left	69.93	−8.91	28.54	
Top right	69.97	−9.10	27.73	
Bottom left	70.14	−8.81	28.71	
Bottom right	70.34	−9.22	27.80	

Transmission at normal incidence: Transmission and reflection of the coating and glass substrate were measured on a Perkin Elmer Lambda 1050 in the range of 200 nm to 2500 nm with a resolution of 10 nm. The sample is placed in front of an integrating sphere to measure the transmission, while the reflection is measured by placing the sample behind the integrating sphere.

Tailored outdoor demonstrator: The tailored-made outdoor demonstrator consists of a steel frame in which four colored and four non-colored black solar panels are mounted. The frame with the solar panels can be tilted by hand to various angles (60°, 45°, 30°, 15°, and 0°). The frame is connected to a base frame which is fixed to two concrete plates (see also Supporting Information S2). The demonstrator is located at the Brightlands Chemelot Campus in Geleen at a shade-free environment with a south–southwest (191°) orientation. The four colored and four black solar panels are connected in series, as can be seen in the schematical drawing of the electrical circuit in Figure 2. Both strings are connected to a DC/AC converter (APS YC100-3), after which the AC electricity is fed into the grid. The DC-generated power of each string is monitored by a QEED QI-power-485-LV measuring the generated current, voltage and power at maximum power point (MPP) (I_{MPP}, V_{MPP}, and P_{MPP}) in one-minute resolution. A Lambrecht Meteo EOLOS-IND weather station containing a pyranometer, temperature and wind sensor was installed at the test location, allowing to translate electrical performance measurements into the power conversion efficiency of the solar panels with respect to the tilt angle. All data are collected in a

cloud which is assessable by InfluxDB version 2.71. Data analysis and visualization were performed by Matplotlib version 3.9.

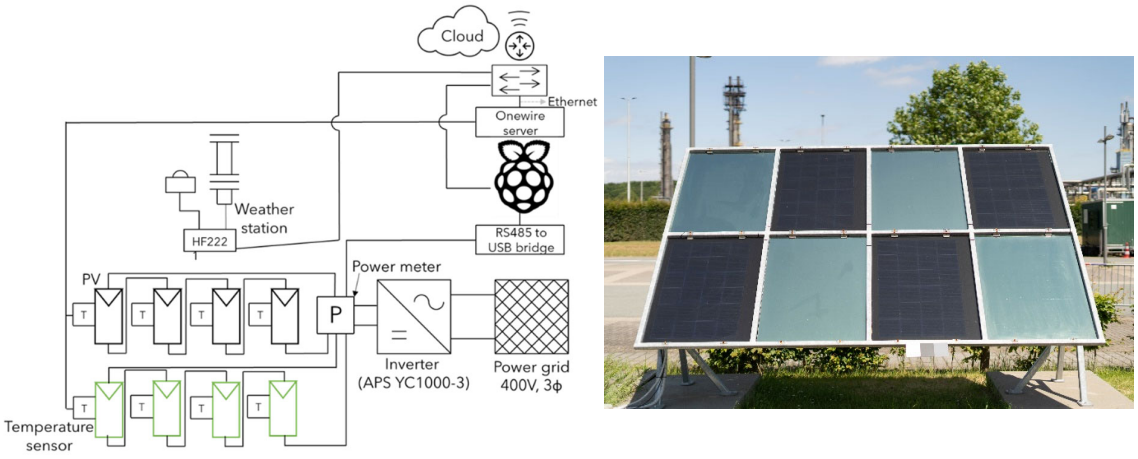

(**a**) (**b**)

Figure 2. (**a**) Schematic illustration of the electrical measurement setup including sensors, hardware and data communication; (**b**) a picture of the demonstrator comprising four colored and four non-colored solar panels.

3. Tailored Measurement Method for Outdoor Color Assessment of Colored PV

Inspired by the work of B. Bläsi et al. [24] and M. Fairchild [36], an outdoor color quantification method has been developed in this study. The method allows to quantify environmental effects on the color appearance of the solar modules such as sunlight intensity, surrounding reflections, and the cloudiness of the sky, along as effects of the viewing angle and tilt angles of the solar panels. Images were taken with a Sony camera (Sony A7 mark III body with a FE 50mm F/1.8 lens) at the viewing angles stated in Figure 3, where 15° tilt is close to horizontal position and 60° tilt is close to vertical orientation. The Sony A7 III camera was selected for its full-frame sensor with a large sensor surface, allowing for increased light capture and higher image quality. This leads to reduced noise and improved color accuracy. All images were captured using a 50 mm lens (Sony FE 50 mm F/1.8). This fixed focal length provides a neutral perspective and is widely applicable to landscape, portrait, and reportage photography, ensuring consistent and reproducible imaging results. The camera was set to manual mode with a fixed ISO value of 100, while all other settings remained constant. The exposure time was varied for each image to maintain a consistently neutral (0) sunlight exposure. The images were also white-balanced in Adobe Lightroom Classic 2019 version 8.4 by means of the greyscale calibration cards attached to the measurement setup (see also Figure 1b). Images were taken at 11 AM on a sunny and cloudy day in May, with a consistent height of the camera of 175 cm. Twenty samples of 250 × 200 pixels were cut out of a picture as indicated by the crosses in Figure 3a, followed by analyzing and averaging the RGB values of all pixels. RGB data is translated to XYZ CIELAB data by Colour Conversion Centre 4.2b for a 10° observer under a D65 light source. This results in 20 CIE XYZ values of the colored solar panels per tilt angle of the measurement setup, viewing angle, and weather condition. The average of these 20 data points is plotted in a chromaticity diagram and exported into an image color file (see the python script in the Supporting Information that is used in this article for color quantification). ΔE 2000 calculations were performed using an online tool to determine the visibility of a color difference for the human eye [37]. Figure 3b shows an

example of three samples taken from an image at 90° viewing angle, 60° tilt angle of the solar panels on a cloudy day. All 20 samples are plotted in a chromaticity diagram.

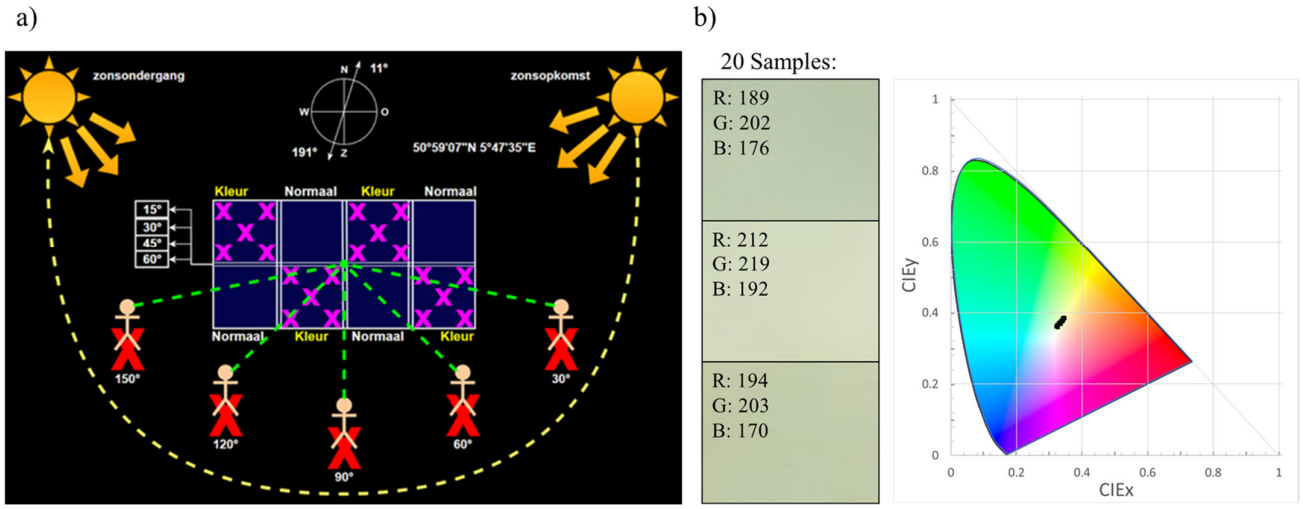

Figure 3. (**a**) Scheme illustrating the developed method for color quantification based on imaging at five different viewing angles, in which the green dotted lines represent the viewing angles and the yellow dotted line represents the solar path; (**b**) an example showing a selection of three samples of 250 × 200 pixels plotted in a chromaticity diagram.

4. Angular Color Measurement Results: Indoor and Outdoor

Angle-dependent transmission: When the position of the sun changes throughout the day and seasons, the angle of incidence of light on a colored solar panel varies, resulting in different transmitted solar spectra through the interference coating. This could potentially result in varying power output and different color observation. Angle-dependent transmission measurements have been performed by OMT Solutions, giving insights into the angular-dependent optical transmission, while transmission and reflection data were measured by TNO-Brightlands Material Center to quantify the transmission and reflection of the coating versus the transmission of bare glass. Figure 4a shows the transmission results for s- and p-polarized light at different transmission angles, where "T0" is the average transmission of s- and p-polarized light measured at normal incidence with respect to the light source and "T60" measured at 60° angle from normal incidence. The transmission spectra of both polarizations were averaged according to Equation (1):

$$T_{coating} = {}^1/_2\left(T_p + T_s\right) \quad (1)$$

where T_s and T_p are the transmissions per wavelength of respectively s- and p-polarized light [38]. Figure 4a shows that the minimal transmission shifts from 540 nm at 0° (normal incidence) to 470 nm at 60° caused by selective reflection of the multilayer interference coating shifting from green to blue light. The effect of selective reflection on the transmission of the coating can be seen in Figure 4b. The transmission of the coating reduces the transmitted solar light through the front glass by a maximum of 41%. Integrating the transmitted solar light intensity shows that up to 78.5% of the solar light power can be transmitted through the coating compared to a bare front glass substrate. It is expected that the electrical output of colored versus non-colored solar panels results in a similar power output reduction up to 21.5%. In addition, Figure 5 shows that the transmitted solar power is very stable with varying transmission angles, which is likely to result in a stable power output with varying tilt angles of the setup. The electrical performance is described later

in this study. The solar light power transmitted through a coating and glass is calculated according to Equation (2):

$$G_{Transmitted\ solar\ light} = \int_{400\text{nm}}^{1100\text{nm}} G(\lambda) \times T_{sample}\, d\lambda \quad (2)$$

where $G(\lambda)$ is the AM1.5G spectrum and T_{sample} is the transmission of the coating or glass.

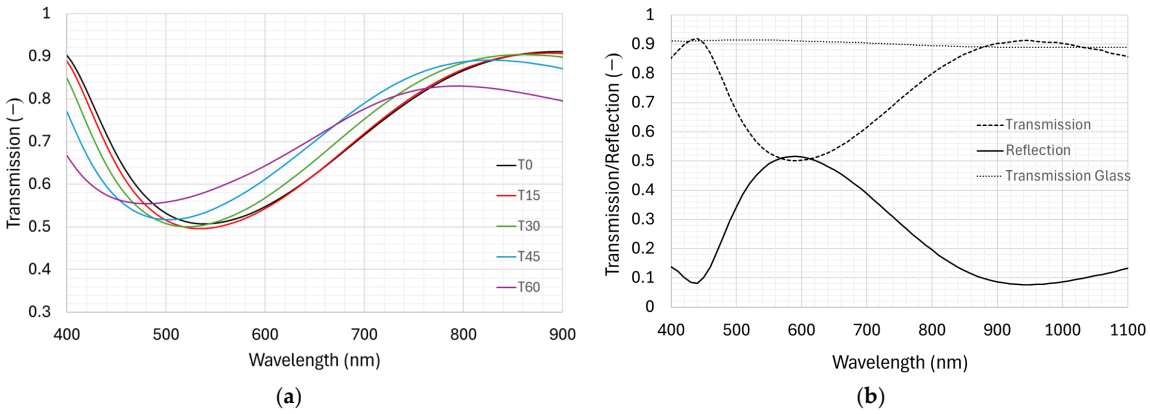

Figure 4. (**a**) Angular dependent average transmission data of p- and s-polarized light; (**b**) transmission and reflection spectra of the interference coating and glass measured in a PerkinElmer Lambda 1050 UV/Vis.

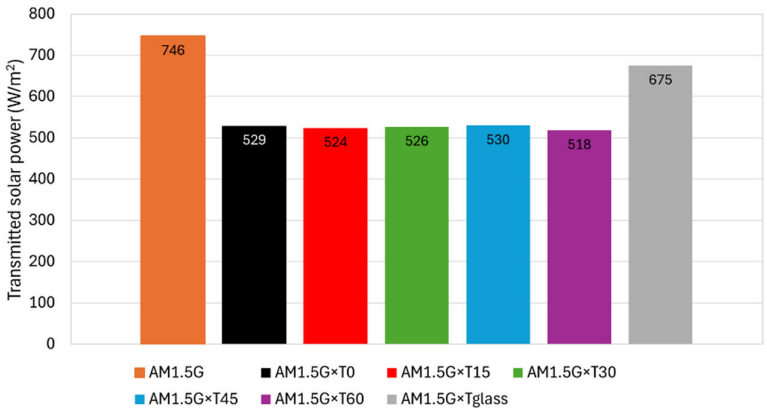

Figure 5. Integrated transmitted solar light through the color coating at multiple angles compared to the intensity of sunlight (orange) and transmitted sunlight through glass (gray).

Outdoor color quantification: Due to the interference effect of the color coating, the perceived color of the module to a viewer is not constant. In this research, a tailored color quantification method has been developed quantifying the color and impact of variables on the perceived color, which is fully described in Section 3. Figure 6 shows all collected data points in a chromaticity diagram for the selected five viewing angles (see also Figure 2), with tilt angles of 60° and 45° (with respect to the horizontal plane) of the solar panels, on both sunny and cloudy days. The data shows that there is a clear difference in perceived color of the solar modules on cloudy and sunny days, where a yellow-green-to-white tint can be observed on cloudy days, and a blue-green-to-white color on sunny days. The two extreme values indicated in Figure 6b correspond to a ΔE of 44.3, indicating a significant visible color difference when the outdoor condition changes from cloudy to sunny. The perceived blue and greenish color is consistent with the measured angular transmission shift from green to blue light presented in Figure 4 and CILAB values presented in Table 1.

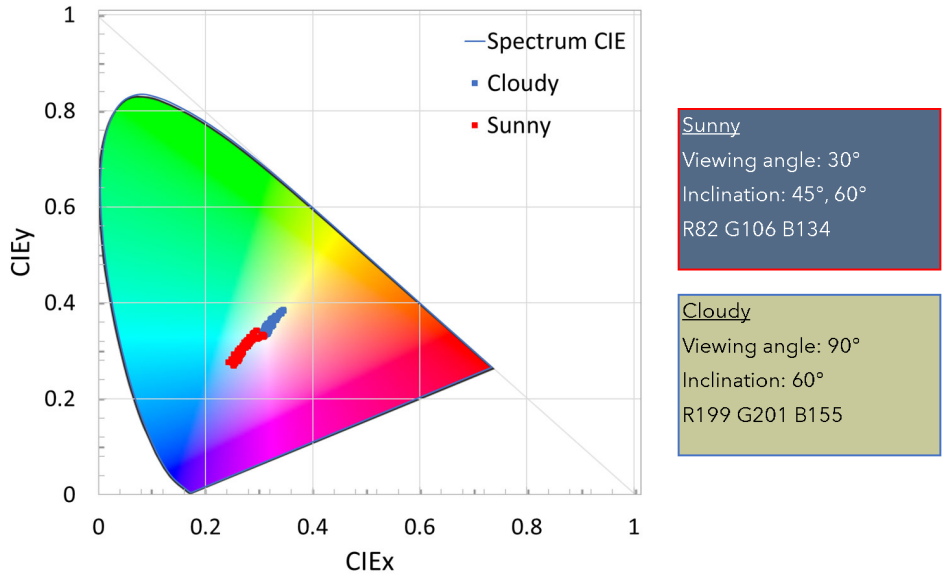

(**a**) (**b**)

Figure 6. (**a**) CIE 1931 spectrum along with all measurement points on sunny days (red) and cloudy days (blue) with viewing angles ranging from 30° to 150° and tilt angles of the test setup of 60° and 45°; (**b**) a visualization of the extreme colors that have been measured.

In addition to the outdoor environment, the tilt angle of the setup influences the color perceived by the viewer. Figure 7 shows the color measurements at a viewing angle of 90°, on a cloudy day, at a tilt angle of 45° and 60°. At a tilt angle of 45° and lower, the aesthetics of the solar modules are influenced by reflection of the sky. On a cloudy day, the white color of the sky is reflected to the viewer, resulting in a whiter appearance of the solar panels. When the tilt angle is increased to 60°, the yellow-green tint of the coating can be perceived by the viewer. At the conditions described in Figure 7, maximum ΔE values of 9.1 and 13.8 for, respectively, 45° and 60° tilt angles are calculated, indicating that the perceived colors are similar with a minor difference with cloudy weather conditions. This effect changes with the viewing angle, where the difference in yellow-green-to-white tint is less pronounced at a larger viewing angle of 120°. On sunny days, the color appearance shows a similar trend, where the blue sky is more reflected towards the viewer at 45° tilt compared to a larger tilt angle of 60°. The chromaticity diagram in Figure 7 shows that at 45°, the measurements are more towards the blue part of the spectrum, while at 60° tilt, the data points shift towards the green part of the spectrum. At small tilt angles, the blue sky on a sunny day is more reflected towards the viewer, while the green-yellow tint of the coating becomes more pronounced at larger tilt angles. At the conditions described in Figure 8, maximum ΔE values of 28.7 and 27.5 for, respectively, 45° and 60° tilt angles are calculated, indicating that the colors observed by a viewer are similar with noticeable difference on a sunny day. The appearance of the coating also changes with the viewing angle, where the effect of sunlight reflection on a sunny day becomes more pronounced with larger viewing angles. Figure 8 shows that under sunny conditions, the solar panels can appear white, caused by direct sunlight reflection. It can be concluded that the developed color quantification method and tailored measurement setup can give insights into the perceived color variation of colored BIPV panels. The results show that the appearance of the coating is affected by the outdoor environment, tilt angle of the test setup and viewing angle. It is likely that the position of the sun also influences the perceived color. This could be investigated in upcoming research.

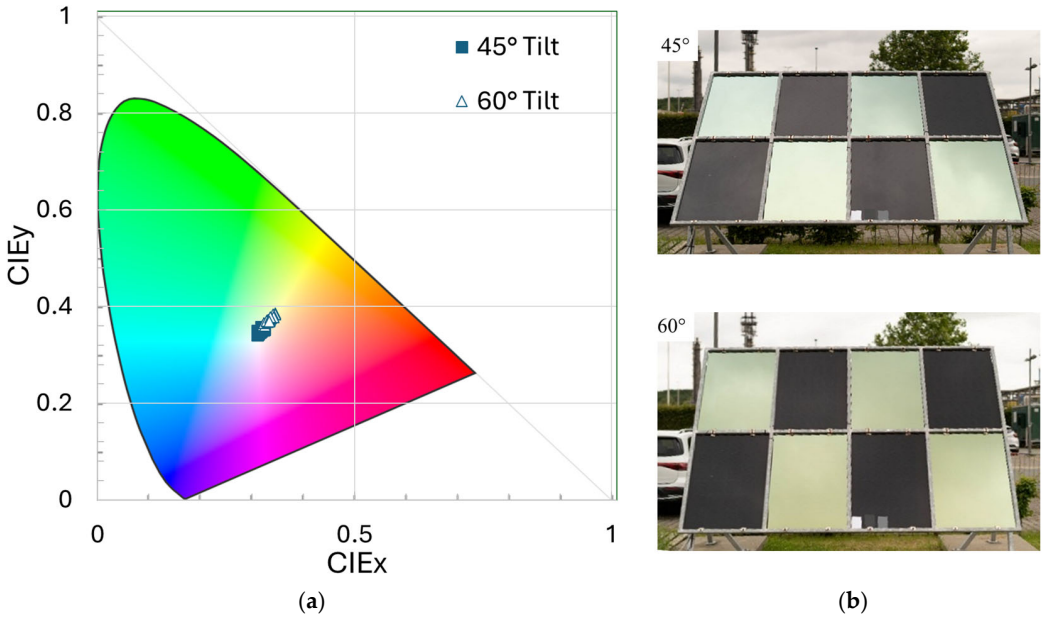

(**a**) (**b**)

Figure 7. (**a**) CIE 1931 spectrum along with the color data measured on a cloudy day, with a viewing angle of 90° and a tilt angle of 45° (closed squares) and 60° (open triangles); (**b**) the images from which the color data were retrieved.

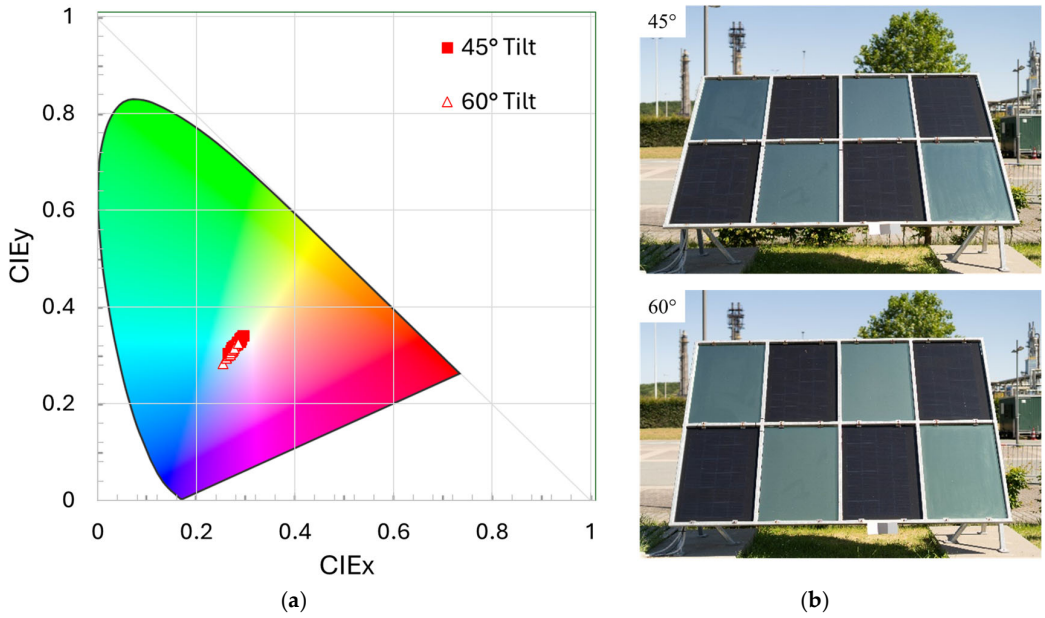

(**a**) (**b**)

Figure 8. (**a**) CIE 1931 spectrum along with the color data measured on a sunny day, with a viewing angle of 90°, with a tilt angle of 45° (closed squares) and 60° (open triangles); (**b**) the images from which the color data were retrieved.

5. Outdoor Electrical Performance Assessment

The effect of the interference coating on the power output of the solar panels has been analyzed at five different tilt angles in a measurement period from April 2024 till September 2024. Per tilt angle, the electrical performance was measured for 3 weeks containing a minimum of three sunny days. Because of the south–southwest orientation of the setup, the sun's position is non-optimal before solar noon. P_{MPP} measurements at the same irradiance levels are therefore lower before solar noon than after solar noon, where the solar panels are more oriented towards the sun, as can be seen in Figure 9. For the analysis of the data

later in this study, a time filter of >13:30 h is used to avoid the effect of the sun's position on power output and efficiency values.

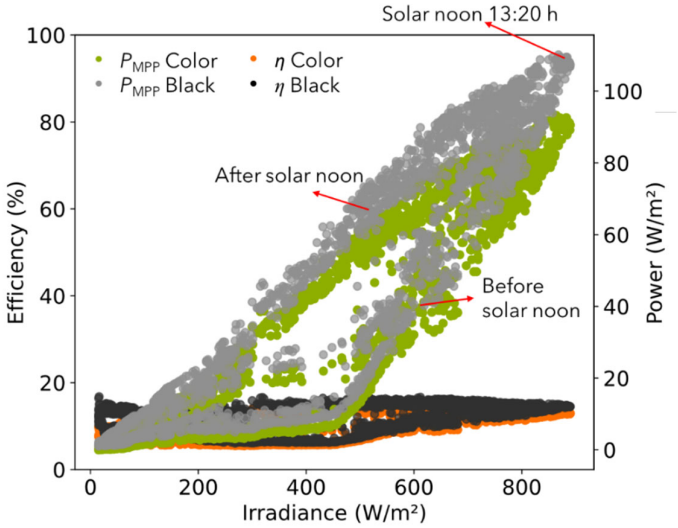

Figure 9. Effect of the sun's irradiance on the efficiency (black, orange) and power output P_{MPP} (gray, green) for colored (orange, green) and black (black, gray) solar panels on three sunny days in May 2024 (1, 11, and 12 May) with a tilt angle of 60°. All data were filtered to an irradiance of ≥15 W/m^2 to avoid outliners due to on/off switching of the inverter.

Figure 10 shows a typical measurement of a sunny day in June with a tilt angle of 30°. At 2 PM, the maximum irradiance of the sun results in a P_{MPP} of 334.5 W (113.0 W/m^2) and 277.5 W (94 W/m^2) for, respectively, the non-colored black and colored solar panels, representing a difference of 17% in power generation between the black and the colored solar panels. Figure 10 shows that the efficiency [η] gradually increases during the day from approximately 8% and 7% at 9AM for black and colored solar panels, respectively, towards 13.1% and 11.2% at 5 PM for black and colored solar panels, respectively. For this specific day, a low power output (<10 W/m^2) is generated before 8 AM and after 8 PM, causing increased inverter losses and a lower signal-to-noise ratio for both power and irradiance measurements, resulting in an increased measurement error. At 16:15, an instant shade (cloud) resulted in an outliner in efficiency. Similar effects of instant shade and low power measurements were observed for another sunny day with a tilt angle of 15° (see Supporting Information S3). Measurements on a sunny day (up to 1000 W/m^2 irradiance) with many clouds show that the irradiance and power measurements are well in line with each other, however, the timing of all data parameters is crucial in obtaining an accurate calculated efficiency.

The power output data presented in Figure 10 is the product of the measured I_{MPP} and V_{MPP} of the black and colored solar panels. Figure 11 shows the current and voltage measurements at maximum power point of the same day as in Figure 10. The results show that the V_{MPP} of the colored and black solar panels is very similar, while the effect of the color coating is significant on the generated current. At maximum generated power, the black and colored solar panels have an I_{MPP} of, respectively, 8545 mA and 7115 mA (or J_{MPP} of 2.89 A/m^2 and 2.40 A/m^2 for black and colored solar panels, respectively). The difference in I_{MPP} between back and colored solar panels corresponds exactly to the 17% difference in power output for this specific day. This result is in between a 12.1% difference measured by a flash test (see Supporting Information S1) and 21.5% reduction in transmitted solar power (Figure 4) for colored versus non-colored solar panels. After sunrise, 07:15 for this specific day, V_{MPP} is at a stable value of 40.2 V. During the day, V_{MPP} gradually decreases to the lowest value of 38.6 V which is likely caused by increasing

outdoor temperature (purple line in Figure 9) and related wafer temperature. Similar results have been obtained for other measurement days with different tilt angles (see Supporting Information S4).

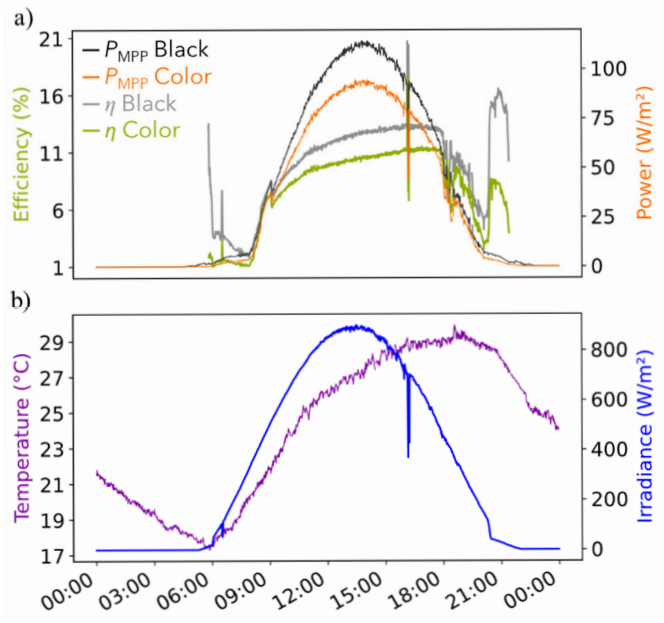

Figure 10. (**a**) Single-day measurements on the 25 June 2024 with a tilt angle of 30° showing the P_{MPP}/m^2 (black) and efficiency (gray) of the non-colored solar panels and P_{MPP}/m^2 (orange) and efficiency (green) for the colored solar panels; (**b**) the irradiance (blue) and outdoor temperature (purple) over time. All data were filtered to irradiance $\geq$ 15 W/m^2 to avoid outliners due to on/off switching of the inverter.

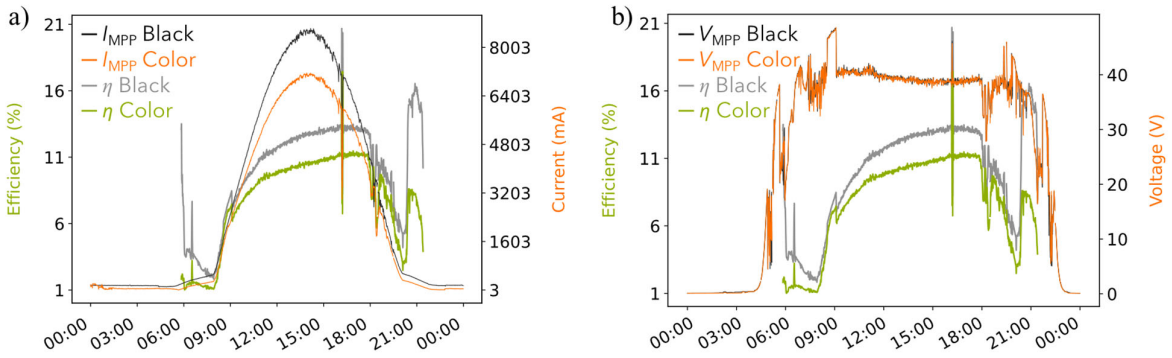

Figure 11. (**a**) Generated current at MPP of black (black) and colored (orange) solar panels along with the efficiency of black (gray) and colored (green) solar panels; (**b**) voltage at MPP of black (black) and colored (orange) solar panels along with the efficiency of black (gray) and colored (green) solar panels. The data has been measured on 25 June 2024 with a tilt angle of 30°. All data was filtered to irradiance $\geq$ 15 W/m^2 to avoid outliners due to on/off switching of the inverter.

Further analysis has been performed to define I_{MPP} at 1000 W/m^2 incident solar radiation by defining the linear relationship between photogenerated current and light intensity at 0° to 60° tilt angles of the solar panels (see Supporting Information S5 for more information). I_{MPP} values at 1000 W/m^2 are 12.8% to 15.5% lower for colored solar panels compared to non-colored solar panels. This reduction in photogenerated current is lower than was expected from the angular transmission data in Figure 4 of 21.5%. This could be attributed to the fact that transmission data was generated at an air/glass interface of the samples while electrical data is retrieved from solar panels with an encapsulant/glass

interface. The difference in interfaces can affect refraction of light and can cause a difference in reflection losses.

To quantify the effect of the interference coating on the power generation of the solar panels, data analysis has been performed over the whole measurement period per tilt angle instead of previous analysis based on single days. Figure 12 shows a bar chart of the summated power generated by the colored and black solar panels over the whole measurement period (approximately 3 weeks per angle). The percentage of power generated by the colored solar panels in relation to the total power generated has been calculated according to Equation (3):

$$\%\ \text{of generated power (color)} = \frac{\sum_{I=15W/m^2}^{I} P_{MPP}(\text{color})}{\sum_{I=15W/m^2}^{I} P_{MPP}(\text{black}) + \sum_{I=15W/m^2}^{I} P_{MPP}(\text{color})} \times 100\% \quad (3)$$

The results show that the colored solar panels generate 9.2% to 10.1% less of the cumulative power than the black solar panels, representing a relative difference of 16.8% to 18.3%. Also, the power conversion efficiency has been analyzed for colored and black solar panels under various tilt angles. Considering all data points after solar noon (see also Figure 9) resulted in a broad standard deviation (σ) on the calculated average efficiency (μ) per tilt angle. Supporting Information S6 shows that the efficiency numbers have σ values of 2.70% on average. The relatively high spread in efficiency data is likely caused by the effect of clouds on efficiency calculations as explained earlier in this study. The effect can be minimized by increasing the irradiance filter from $\geq$15 W/m^2 to $\geq$500 W/m^2. Increasing the irradiance filter to such a high solar irradiance level does not result in statistical limitations, since still over 1900 data points are collected as shown in Table 2. However, outliers caused by clouds can be excluded, leading to acceptable σ values. The results show that solar panels with a color coating have a reduced relative efficiency between 14.1% and 15.7%, with an average absolute difference of 1.8%. This result is in line with previously analyzed I_{MPP} and P_{MPP} data. Somewhat lower power conversion efficiency (PCE) is measured in the outdoor measurement setup compared to lab data retrieved by flash tests (Supporting Information S1). This can be attributed to temperature effects, soiling effect, cabling losses and inverter losses. Efficiency values at 60°, 45°, 30° and 15° tilt angles are very close to each other, as can be expected according to Hespul's table for the Netherlands, with decreasing efficiency at 15° and 0° tilt angles. The colored solar panels with the multilayer interference coating do not show an angular-dependent power output, which could also be expected from the angular transmission measurements (described in Figure 4), which is an interesting and beneficial feature of the developed color coating.

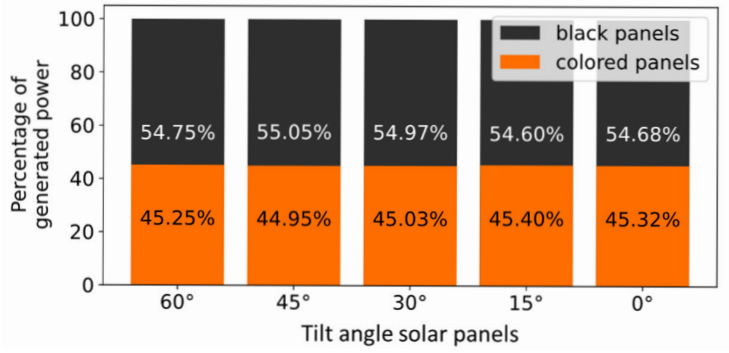

Figure 12. Relative accumulated power generated by the black (black) and colored (orange) solar panels under various tilt angles. Data filter of irradiance $\geq$ 15 W/m^2 was applied.

Table 2. Statistical information about the calculated efficiency values presented in Figure 13 showing the amount of data points, average efficiency (μ), standard deviation (σ) and the relative and absolute efficiency difference between black and colored PV panels. Data filters of irradiance ≥500 W/m^2 and timestamp >13:30 h were applied.

Tilt Angle	Black/Color	Data Points	μ (%)	σ	Δμ (%) Absolute	Δμ (%) Relative
60°	Black	2267	12.78	1.57	1.91	−14.96
	Color		10.87	1.36		
45°	Black	1933	12.61	1.84	1.95	−15.43
	Color		10.66	1.57		
30°	Black	2830	12.71	1.66	2.00	−15.72
	Color		10.71	1.42		
15°	Black	2305	12.40	0.96	1.91	−15.43
	Color		10.49	0.85		
0°	Black	3411	9.45	3.52	1.33	−14.09
	Color		8.12	3.03		

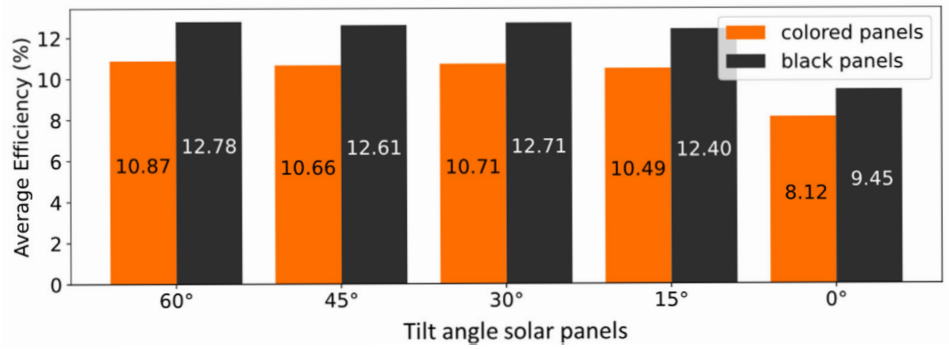

Figure 13. Conversion efficiency of the black (black) and colored (orange) solar panels under various tilt angles. Data filter of irradiance ≥500 W/m^2 was applied and timestamp >13:30 h was applied.

6. Conclusions and Outlook

In this research, a tailored outdoor measurement setup and method were developed which proved their value to quantify angular-dependent color appearance along with the angular-dependent electrical power output in an outdoor environment. By means of photography followed by white balancing, sample cutting, averaging the RGB values of all pixels per sample, and calculating the XYZ CIELAB values, a variation in color appearance can be plotted in chromaticity diagrams. These diagrams can give valuable insights into the angular stability and effects of climate conditions on the color appearance of colored BIPV products. For the specific solar panels analyzed in this study, the color perception to a viewer is influenced by the environmental conditions, where a yellow-green color appears on cloudy days and a blue-green color on sunny days. Reflection of the sun or clouds at specific viewing and tilt angles can result in a white appearance of the modules. Next to the color appearance, the tailored measurement setup allowed to monitor the performance of the colored solar panels versus non-colored solar panels in an outdoor environment with different tilt angles. Taking into account all measured data points, a maximal difference in power output of 18.3% was measured. When only sunny days are taken into account, leaving out the measurement data obtained at low irradiance (<500 W/m^2), the relative difference in power output reaches only up to 15.7% between colored and non-colored solar modules. As 84.3% of the power output can be retained

with the multilayer interference coloring technique, and the effect of the color coating on the performance of the solar panels is not angular-dependent, the developed coating has interesting potential for colored PV applications. In this work, the color analysis method and electrical performance study is demonstrated on a small number of solar panels at one specific location with limited seasonal variation. Monitoring of mid-sized installations over a full year at different locations should be carried out to verify the results. The color variation of the solar module could be an interesting feature to increase the integration of the solar module into its surroundings. Additional research should be carried out into the social acceptance and architectural integration of the colored solar modules. In future work, the tailored measurement setup and developed measurement method will be used for comparative studies on various coloring techniques.

Supplementary Materials: The following supporting information can be downloaded at https://www.mdpi.com/article/10.3390/buildings16122357/s1, Figure S1: (a) Front and (b) back view of the Kameleon Solar PV panels showing the specific dimensions. Table S1: Electrical properties of the colored and black solar panels measured by Kameleon Solar with a flash test. Figure S2: Three-dimensional image showing the construction of the outdoor demonstrator. Figure S3: (a,c) Single-day measurements on a sunny day at 11 August 2024 and (b,c) on a sunny day with many clouds at 23 June 2024, showing (a,b) P_{MPP}/m^2 and efficiency, along with (b,d) irradiance and outdoor temperature of colored and black solar panels. All data were filtered to irradiance $\geq$15 W/m^2 to avoid spikes by on/off switching of the inverter. Figure S4: (a) Generated current at MPP (black, orange) along with the efficiency (green, gray) of black (black, gray) and colored (orange, green) solar panels. (b) Voltage at MPP (black, orange) along with the efficiency (green, gray) of black (black, gray) and colored (orange, green) solar panels. The data has been measured on 28 August 2024 with a tilt angle of 0°. (c,d) Outdoor temperature (purple) and irradiance (blue). All data were filtered to irradiance $\geq$15 W/m^2 to avoid outliners due to on/off switching of the inverter. Figure S5: (a) Generated current at MPP (black, orange) along with the efficiency (green, gray) of black (black, gray) and colored (orange, green) solar panels. (b) Voltage at MPP (black, orange) along with the efficiency (green, gray) of black (black, gray) and colored (orange, green) solar panels (b). The data has been measured on 12 May 2024 with a tilt angle of 60°. (c,d) Outdoor temperature (purple) and irradiance (blue). All data were filtered to irradiance $\geq$15 W/m^2 to avoid outliners due to on/off switching of the inverter. Figure S6: Effect of irradiance on power (gray, orange) and current (grey, red) measured on three sunny days with a tilt angle of (a,b) 0°, (c,d) 15°, (e,f) 30°, (g,h) 45° and (i,j) 60°. A time filter of >13:30 h has been applied along with an irradiance filter of $\geq$15 W/m^2. Table S2: I_{MPP} and P_{MPP} of black and colored solar panels extrapolated to 1000 W/m^2. Figure S7: Conversion efficiency of the black (black) and colored (orange) solar panels under various tilt angles. Data filter of irradiance $\geq$15 W/m^2 was applied and timestamp >13:30 h was applied. Table S3: Statistical information about the calculated efficiency values presented in Figure 8 showing the amount of data points, average efficiency (μ), standard deviation (σ) and the relative and absolute performance loss due to the application of a color coating. Data filter of irradiance $\geq$15 W/m^2 was applied and a timestamp >13:30 h was applied.

Author Contributions: Conceptualization, M.A.A., P.v.N., S.T., D.M., P.B., Z.V. and F.C.; methodology, M.A.A. and R.H.; software, M.A.A. and R.D.; validation, M.A.A., D.M., P.B., Z.V. and F.C.; formal analysis, M.A.A. and R.D.; investigation, M.A.A., R.D., R.H., P.v.N., S.T., D.M., C.P.K.Y., C.R. and F.C.; resources, C.R.; data curation, M.A.A. and R.D.; writing—original draft preparation, M.A.A. and F.C.; writing—review and editing, R.D., R.H., P.v.N., S.T., D.M., P.B., C.R. and Z.V.; visualization, M.A.A., R.D., R.H., P.v.N., S.T., C.P.K.Y. and C.R.; supervision, D.M. and F.C.; project administration, P.B. and Z.V.; funding acquisition, D.M., P.B. and Z.V. All authors have read and agreed to the published version of the manuscript.

Funding: We would like to thank Europees Fonds voor Regionale Ontwikkeling (EFRO) for funding the LEEF project within the OPZuid program.

Data Availability Statement: The data presented in this study is available on request.

Acknowledgments: We would like to thank Prinz Optics for applying the developed coating formulation on the solar glass sheets and thereby making an important transition from lab- to large-scale production.

Conflicts of Interest: OMT Solutions was involved in this study for their expertise in optical measurements. At OMT Solutions, angular-dependent transmission measurements were performed of the developed colored coatings. Kameleon Solar was involved in the electrical design and production of the colored solar panels. At Kameleon Solar, the solar panels were analyzed under standard test conditions, which served as a reference point in the outdoor performance analysis study.

References

1. European Union Directive (EU). *2024/1275 of the European Parliament and of the Council of 24 April 2024 on the Energy Performance of Buildings (Recast)*; European Union: Luxembourg, 2024; Volume 1275.
2. European Union. *Regulation (EU) 2021/1119 of the European Parliament and of the Council of 30 June 2021 Establishing the Framework for Achieving Climate Neutrality and Amending Regulations (EC) No 401/2009 and (EU) 2018/1999 ('European Climate Law')*; European Union: Luxembourg, 2021.
3. European Commision. *Communication from the Commission to the European Parliament, the Council, the European Economic and Social Committee and the Committee of the Regions "Fit for 55": Delivering the EU's 2030 Climate Target on the Way to Climate Neutrality*; European Commision: Brussels, Belgium, 2021.
4. European Commision. *Communication from the Commission to the European Parliament, the European Council, the Council, the European Economic and Social Committee and the Committee of the Regions RepowerEU Plan*; European Commision: Brussels, Belgium, 2022.
5. Ghorayeb, R.; van der Ree, B.; Benninga, J.; van Beek, A. *High Level Energy Efficiency Guidelines for Building Reconstruction and Upgrades in Lebanon*; LELC: Beirut, Lebanon, 2021.
6. Marc, J.; Puguan, C.; Rathod, P.V.; Chavan, P.V.; Lee, J.; Kim, H. Solar Light Modulating Materials for Energy Efficient Smart Window Design: Recent Trends and Future Perspectives. *Sol. Energy Mater. Sol. Cells* **2025**, *282*, 113407. [CrossRef]
7. Mann, D.; Yeung, C.; Habets, R.; Vroon, Z.; Buskens, P. Comparative Building Energy Simulation Study of Static and Thermochromically Adaptive Energy-Efficient Glazing in Various Climate Regions. *Energies* **2020**, *13*, 2842. [CrossRef]
8. Dungani, R.; Hua, L.S.; Chen, L.W.; Nurani, W.; Solihat, N.N.; Maulani, R.R.; Dewi, M.; Aditiawati, P.; Fitria; Antov, P.; et al. Potential of Lignin and Cellulose as Renewable Materials for the Synthesis of Flame-Retardant Aerogel Composites. *Mater. Today Commun.* **2024**, *41*, 110501. [CrossRef]
9. Mao, T.; Xie, S.; Chen, L.; Xiao, H.; Wang, P. High-Strength, Flame-Retardant, Hydrophobic and UV-shielding Cellulose Aerogel Modified with Xylooligosaccharide-Derived Crosslinker and Methyltrimethoxysilane. *Polym. Degrad. Stab.* **2025**, *240*, 111492. [CrossRef]
10. De Leede, G.; Rechter, M.; van Rensburg, J.J.; Hamm, M.; van Os, J.-J.; van Erp, L.; Derks, R.; Westerdijk, R.; Jeeninga, H.; Heller, R.; et al. *Circulaire Geïntegreerde Hoog-Rendements Zonnepanelen*; AMOLF: Amsterdam, The Netherlands, 2023.
11. European Commision. *Communication from the Commission to the European Parliament, the Council, the European Economic and Social Committee and the Committee of the Regions EU Solar Energy Strategy*; European Commision: Brussels, Belgium, 2022.
12. International Energy Agency (IEA). *Renewables 2024 Analysis and Forecast to 2030*; International Energy Agency (IEA): Paris, France, 2024.
13. Defaix, P.R.; van Sark, W.G.J.H.M.; Worrell, E.; de Visser, E. Technical Potential for Photovoltaics on Buildings in the EU-27. *Sol. Energy* **2012**, *86*, 2644–2653. [CrossRef]
14. Molnár, G.; Cabeza, L.F.; Chatterjee, S.; Ürge-Vorsatz, D. Modelling the Building-Related Photovoltaic Power Production Potential in the Light of the EU's Solar Rooftop Initiative. *Appl. Energy* **2024**, *360*, 122708. [CrossRef]
15. Van Hooff, W.; Kuijers, T.; Quax, R.; Witte, J. *Ruimtelijk Potentieel van Zonnestroom in Nederland*; TKI Urban Energy: Utrecht, The Netherlands, 2021.
16. Sterchele, P.; Brandes, J.; Heilig, J.; Wrede, D.; Kost, C.; Schlegl, T.; Bett, A.; Henning, H. *Paths to a Climate-Neutral Energy System the German Energy Transition in Its Social Context 27%*; Fraunhofer ISE: Freiburg, Germany, 2020.
17. Bódis, K.; Kougias, I.; Jäger-waldau, A.; Taylor, N.; Szabó, S. A High-Resolution Geospatial Assessment of the Rooftop Solar Photovoltaic Potential in the European Union. *Renew. Sustain. Energy Rev.* **2019**, *114*, 109309. [CrossRef]
18. Borja Block, A.; Escarre Palou, J.; Courtant, M.; Virtuani, A.; Cattaneo, G.; Roten, M.; Li, H.Y.; Despeisse, M.; Hessler-Wyser, A.; Desai, U.; et al. Colouring Solutions for Building Integrated Photovoltaic Modules: A Review. *Energy Build.* **2024**, *314*, 114253. [CrossRef]

19. Corti, P.; Bonomo, P.; Frontini, F.; Macé, P.; Bosch, E. *Building Integrated Photovoltaics: A Practical Handbook for Solar Buildings' Stakeholders Status Report*; Istituto Sostenibilità Applicata All'ambiente Costruito (ISAAC): Mendrisio, Switzerland, 2020.
20. Kuhn, T.E.; Erban, C.; Heinrich, M.; Eisenlohr, J.; Ensslen, F.; Neuhaus, D.H. Review of Technological Design Options for Building Integrated Photovoltaics (BIPV). *Energy Build.* **2021**, *231*, 110381. [CrossRef]
21. Jolissaint, N.; Hanbali, R.; Hadorn, J.C.; Schüler, A. Colored Solar Facades for Buidlings. *Energy Procedia* **2017**, *122*, 175–180. [CrossRef]
22. Ben Amara, M.; Balghouthi, M. Colored Filter's Impact on the Solar Cells' Electric Output under Real Climatic Conditions for Application in Building Integrated Photovoltaics. *J. Build. Eng.* **2023**, *76*, 107276. [CrossRef]
23. Borja Block, A.; Escarre Palou, J.; Faes, A.; Virtuani, A.; Ballif, C. Accurate Color Characterization of Solar Photovoltaic Modules for Building Integration. *Sol. Energy* **2024**, *267*, 112227. [CrossRef]
24. Blasi, B.; Kroyer, T.; Kuhn, T.; Hohn, O. The MorphoColor Concept for Colored Photovoltaic Modules. *IEEE J. Photovolt.* **2021**, *11*, 1305–1311. [CrossRef]
25. Schüler, A.; Dutta, D.; de Chambrier, E.; Roecker, C.; De Temmerman, G.; Oelhafen, P.; Scartezzini, J.L. Sol-Gel Deposition and Optical Characterization of Multilayered $SiO_2/Ti_{1-X}Si_xO_2$ Coatings on Solar Collector Glasses. *Sol. Energy Mater. Sol. Cells* **2006**, *90*, 2894–2907. [CrossRef]
26. Soman, A.; Antony, A. Colored Solar Cells with Spectrally Selective Photonic Crystal Reflectors for Application in Building Integrated Photovoltaics. *Sol. Energy* **2019**, *181*, 1–8. [CrossRef]
27. Manwani, K.; Lagier, M.; Krammer, A.; Fleury, J.; Schüler, A. Development of Novel Orange Colored Photovoltaic Modules with Improved Angular Stability and High Energy Efficiency. *Sol. Energy Mater. Sol. Cells* **2024**, *278*, 113144. [CrossRef]
28. Li, Z.; Ma, T.; Yang, H.; Lu, L.; Wang, R. Transparent and Colored Solar Photovoltaics for Building Integration. *Sol. RRL* **2021**, *5*, 2000614. [CrossRef]
29. Rudzikas, M.; Donėlienė, J.; Bužavaitė-Vertelienė, E.; Balevičius, Z.; Leuvrey, C.; Šetkus, A. Design and Investigation of 1D Photonic Crystal Based Structures for BIPV Cell Colorization by Sol-Gel Dipping Technology. *Sol. Energy* **2023**, *250*, 285–294. [CrossRef]
30. Technology @ Colorquant.Cc. Available online: https://colorquant.cc/en/technology (accessed on 23 April 2026).
31. Technology @ Kromatix.Com. Available online: https://kromatix.com/technology (accessed on 23 April 2026).
32. Abdullah, M.; Hosain, M.M.; Hassan Parvez, M.M.; Haque Motayed, M.S. Prospects and Challenges of Thin Film Coating Materials and Their Applications. *Inorg. Chem. Commun.* **2025**, *175*, 114117. [CrossRef]
33. Attia, S.M.; Wang, J.; Wu, G.; Shen, J.; Ma, J. Review on Sol-Gel Derived Coatings: Process, Techniques and Optical Applications. *J. Mater. Sci. Technol.* **2002**, *18*, 3.
34. Butt, M.A. Thin-Film Coating Methods: A Successful Marriage of high-quality and cost-effectiveness—A brief exploration. *Coatings* **2022**, *12*, 1115. [CrossRef]
35. Habets, R.; Vroon, Z.; Erich, B.; Meulendijks, N.; Mann, D.; Buskens, P. Structural Color Coatings for High Performance BIPV. *IOP Conf. Ser. Earth Environ. Sci.* **2021**, *855*, 5. [CrossRef]
36. Fairchild, M.D. Color Appearance Models and Complex Visual Stimuli. *J. Dent.* **2010**, *38*, 25–33. [CrossRef]
37. Kleurverschilcalculator | RapidToolSet. Available online: https://rapidtoolset.com/nl/tool/color-difference-calculator (accessed on 2 June 2026).
38. Smith, G.B.; Dligatch, S.; Sullivan, R.; Hutchins, M.G. Thin Film Angular Selective Glazing. *Sol. Energy* **1998**, *62*, 229–244. [CrossRef]

Disclaimer/Publisher's Note: The statements, opinions and data contained in all publications are solely those of the individual author(s) and contributor(s) and not of MDPI and/or the editor(s). MDPI and/or the editor(s) disclaim responsibility for any injury to people or property resulting from any ideas, methods, instructions or products referred to in the content.